

Stratospheric aerosol injection to stabilize Northern Hemisphere terrestrial permafrost under the ARISE-SAI-1.5 scenario

Ariel Lena Morrison¹, Elizabeth A. Barnes¹, and James Wilson Hurrell¹

¹Colorado State University

September 27, 2023

1 **Stratospheric aerosol injection to stabilize Northern**
2 **Hemisphere terrestrial permafrost under the**
3 **ARISE-SAI-1.5 scenario**

4 **A. L. Morrison¹, E. A. Barnes¹, and J. W. Hurrell¹**

5 ¹Department of Atmospheric Sciences, Colorado State University, Fort Collins, CO, USA

6 **Key Points:**

- 7 • Stratospheric aerosol injection is unlikely to fully stabilize permafrost extent by
8 2069 despite maintaining permafrost temperature
- 9 • Stratospheric aerosol injection could prevent nearly all talik formation compared
10 to SSP2-4.5
- 11 • Near-zero net changes in carbon stocks are projected in total permafrost and per-
12 mafrost peat regions after stratospheric aerosol injection

Corresponding author: A. L. Morrison, ariel.morrison@colostate.edu

13 Abstract

14 Permafrost, or ground that is continuously frozen for at least two years, contains vast
15 stores of organic soil carbon. Stratospheric aerosol injection (SAI) may prevent tipping
16 points that lead to widespread permafrost thaw and carbon release by cooling surface
17 and soil temperatures, but it is unclear if or when permafrost could stabilize after SAI
18 deployment. Here we use output from the ARISE-SAI-1.5 simulations to assess how per-
19 mafrost may respond to a specific SAI strategy that maintains global mean surface tem-
20 perature to 1.5°C above pre-industrial levels. Permafrost responses under SAI are com-
21 pared to responses under the control SSP2-4.5 emissions scenario. We show that the rate
22 of boreal permafrost thaw slows under SAI but does not fully stop, likely due to deep
23 permafrost thaw processes that are resistant to surface temperatures changes. In both
24 the ARISE-SAI-1.5 and SSP2-4.5 simulations, permafrost completely thaws and disap-
25 pears along the southern edge of the permafrost area by 2069, indicating that some com-
26 plete thaw may be inevitable even if SAI successfully stabilizes global mean surface tem-
27 peratures. SAI does prevent a potential tipping point (talik formation) in roughly 1 mil-
28 lion km² of permafrost, most of which is located in permafrost peatlands. Thus, a more
29 aggressive SAI strategy than that of ARISE-SAI-1.5 is likely required to prevent all fu-
30 ture projected permafrost thaw.

31 Plain Language Summary

32 Permafrost is ground that stays frozen for at least two years. Permafrost thaw is
33 a global concern because of how much soil carbon it stores, which can be released into
34 the atmosphere as carbon dioxide and methane if permafrost thaws. One proposed method
35 that could prevent permafrost thaw is to cool the Earth by injecting reflective particles
36 into the stratosphere, which would block a small percentage of incoming sunlight and
37 stabilize Earth's temperature to 1.5°C above pre-industrial temperatures. We use climate
38 projections from an Earth system model to assess how permafrost might respond to a
39 proposed scenario for stabilizing Earth's temperature. We find that the total amount of
40 permafrost still decreases even in a scenario where the Earth's temperature has stabi-
41 lized, but pockets of unfrozen soil within and above permafrost are less likely to form,
42 which reduces the possibility of rapid and widespread permafrost thaw. A climate in-
43 tervention strategy that starts sooner or aims to cool the Earth more may be required

44 in order to fully prevent future permafrost thaw and associated carbon dioxide and methane
45 emissions.

1 Introduction

We are not on track to meet the Paris Climate Agreement goal of limiting warming to below 2°C (Pihl et al., 2019). Rising global temperatures increases the likelihood of reaching tipping points in the climate system, or positive feedbacks that accelerate warming (Armstrong McKay et al., 2022; Lenton, 2012). While CO₂ removal and reduced dependence on fossil fuels are preferred ways to prevent possible critical climate conditions that lead to tipping points, the speed and intensity of ongoing climate changes might necessitate direct climate intervention. Stratospheric aerosol injection (SAI) is a hypothetical solar radiation management (SRM) strategy (Keith, 2000) that would increase Earth's albedo and stabilize or reduce surface temperatures by injecting highly reflective particles into the stratosphere (Rasch et al., 2008). If deployed, SAI could potentially mitigate some climate change impacts (e.g., Chen et al., 2020; Dagon & Schrag, 2017), although the full range of possible impacts has not yet been established. One region of particular concern is the Arctic, which is currently warming several times faster than the global average (Rantanen et al., 2022) and has many potential positive feedbacks, such as permafrost thaw.

Permafrost is ground that is continually below 0°C for at least two years. Permafrost thaw is a regional and global concern because of the carbon stores in permafrost soils: it is estimated that the northern circumpolar permafrost zone contains ~1,460-1,600 Pg carbon (Hugelius et al., 2014; Schuur et al., 2015), or twice as much carbon as is in the atmosphere (Schuur et al., 2018). Permafrost peatlands contain ~12% of the total soil organic carbon stored in northern boreal permafrost (Hugelius et al., 2020), and the carbon released from peatlands can be released as CO₂ or CH₄ (Swindles et al., 2015; Voigt et al., 2019). This carbon loss can occur on the scale of years-to-decades, although it may take centuries for peatlands to regain pre-thaw carbon stores (Fewster et al., 2022; Heffernan et al., 2020; Jones et al., 2016; Manies et al., 2021). Some of the loss could be offset by increased productivity and peat accumulation in warmer conditions (Heffernan et al., 2020; Swindles et al., 2015; Treat et al., 2021). Under moderate warming scenarios, permafrost peatland area is projected to decrease by 75-90% by the 2060s (Fewster et al., 2022; Könönen et al., 2023), and may soon reach a tipping point that leads to rapid and widespread thaw.

77 Talik, or perennially unfrozen soil within or above permafrost, may be a precursor
78 to both widespread permafrost thaw (Schuur et al., 2008) and permafrost soils transitioning
79 from a carbon sink to a carbon source (Connon et al., 2018; Devoie et al., 2019;
80 Farquharson et al., 2022; Parazoo et al., 2018). Permafrost tipping points are difficult
81 to quantify and generally refer to the onset of widespread permafrost thaw (Lenton, 2012),
82 so talik formation, as a precursor to widespread thaw, may be considered a quantifiable
83 indication of an imminent permafrost tipping point. Therefore, it is important to understand
84 when and where talik may form in the future.

85 Previous work has shown that different climate intervention strategies could slow
86 the rate and extent of permafrost thaw (Chen et al., 2023; H. Lee et al., 2019; W. Lee
87 et al., 2023; Liu et al., 2023) and reduce carbon emissions from permafrost soils (Chen
88 et al., 2020, 2023; W. Lee et al., 2023; Liu et al., 2023), but these studies did not separate
89 permafrost response by land type or assess specific forms of permafrost degradation
90 such as talik formation. The goal of this study is to assess whether a specific SAI
91 strategy might stabilize existing Northern Hemisphere terrestrial permafrost and prevent
92 future critical climate conditions such as talik formation that could lead to widespread
93 accelerated thaw and carbon release.

94 **2 Data and Methods**

95 **2.1 ARISE-SAI-1.5 simulations**

96 The Assessing Responses and Impacts of Solar climate intervention on the Earth
97 system with Stratospheric Aerosol Injection (ARISE-SAI) project is a set of Earth system
98 simulations that was designed to assess the potential risks and benefits of a specific
99 SRM protocol (Richter et al., 2022). The ARISE-SAI simulations were run with the Community
100 Earth System Model version 2 (CESM2; Danabasoglu et al. (2020)) on a 0.9 x
101 1.25° horizontal resolution grid with the Whole Atmosphere Community Climate Model
102 version 6 (WACCM6; Gettelman et al. (2019)) as the atmospheric component and the
103 Community Land Model version 5 (CLM5; Lawrence et al. (2019)) as the land component.
104 While CESM2 does not specifically include a permafrost model, its land model component
105 has updated snow density, soil biogeochemistry, and soil hydrology to more accurately
106 simulate permafrost dynamics compared with previous versions of CLM (Lawrence
107 et al., 2019). The soil column in CLM5 has 25 layers of variable thickness that extend

108 to nearly 50 m depth. Only the top 20 layers, down to 8.6 m, can be soil; the remain-
109 ing five layers are bedrock. The bedrock depth in CLM5, however, is spatially variable
110 and ranges from 8.6 m at its deepest to < 1 m at its shallowest (Lawrence et al., 2018,
111 2019). The only hydrologically and biogeochemically active layers of the soil column are
112 the layers above the bedrock.

113 We use the 10-member ensemble of ARISE-SAI-1.5 simulations, in which sulfur diox-
114 ide (SO_2) is injected into the stratosphere at ~ 21.5 km altitude at 15° and 30°N/S along
115 180°E . The initial aerosol injection is in 2035, and the simulation runs for 35 years un-
116 til 2069. Every year, a feedback-control algorithm (MacMartin et al., 2014; Kravitz et
117 al., 2017) in ARISE-SAI-1.5 adjusts how much aerosol is injected from each of the four
118 locations in an effort to meet three climate objectives: maintain global mean temper-
119 ature increase at 1.5°C above pre-industrial levels, maintain the north-south surface tem-
120 perature gradient, and maintain the Equator-to-pole surface temperature gradient, all
121 under the Shared Socioeconomic Pathway 2 (SSP2)-4.5 emissions scenario (Riahi et al.,
122 2017). In order to assess climate outcomes in a potential SAI vs non-SAI world, we com-
123 pare the climate outcomes in ARISE-SAI-1.5 with a 10-member ensemble of SSP2-4.5
124 reference (or control) simulations also run from 2015–2069.

125 2.2 Permafrost data

126 Permafrost exists in CLM5 where there is an active layer, or ground that season-
127 ally thaws and re-freezes. Since we are interested in the biogeochemically active permafrost
128 (i.e., permafrost that can release carbon when it thaws), we restrict permafrost to only
129 the grid cells where the maximum annual active layer thickness (ALTMAX) is shallower
130 than the bedrock depth. That is, ALTMAX must be < 8.6 m. A shallower active layer
131 means that the near-surface soil remains frozen, while a deeper active layer indicates that
132 the region is warmer and the underlying permafrost is likely more degraded and less re-
133 sponsive to surface changes in temperature or precipitation. To our knowledge, this is
134 the first study that uses a variable depth limit for ALTMAX and permafrost based on
135 a variable bedrock depth. We use ALTMAX to find annual permafrost extent, and the
136 annual mean active layer depth (ALT) in calculations for permafrost volume and tem-
137 perature. Permafrost volume in each grid cell is calculated as the depth of soil between
138 the bottom of the active layer and the top of the bedrock in each cell, multiplied by each
139 grid cell's area. Permafrost temperature is a weighted average of the soil temperature

140 between the bottom of the active layer and the top of the bedrock in each grid cell, where
141 the thickness of each soil layer is the weight.

142 While talik is not often assessed in climate models due to their relatively coarse
143 horizontal and vertical resolution, Parazoo et al. (2018) provide a framework for find-
144 ing talik in CESM2 and we use their definition here. The timing of talik formation is the
145 first year when the monthly mean soil temperature (TSOI) in any subsurface layer down
146 to the bedrock exceeds -0.5°C for the entire calendar year (January–December; based on
147 the freeze-thaw threshold from Parazoo et al. (2018)). The soil layer must consistently
148 remain above -0.5°C for at least two years. Talik formation is restricted to permafrost
149 regions.

150 Finally, we use changes in total ecosystem carbon (ΔECOC ; units gC m^{-2}) to as-
151 sess changes in total carbon stocks in the boreal permafrost area over time. ΔECOC ac-
152 counts for changes in vegetation, leaf and root litter, and soil carbon (Lawrence et al.,
153 2019). ΔECOC allows us to see the yearly balance between increasing land carbon through
154 plant growth, and decreasing land carbon through emissions from decomposition in thaw-
155 ing permafrost. ΔECOC is calculated for each year relative to 2035 values in SSP2-4.5
156 and ARISE-SAI-1.5. It is only assessed in the grid cells that contain permafrost each year,
157 so each year the area for which ECOC is calculated may be different. Therefore, we re-
158 port ΔECOC in units of gC m^{-2} instead of reporting the ΔECOC in total gC for the en-
159 tire permafrost area.

160 **2.3 Land type**

161 We show some permafrost changes in the context of land type, specifically peat-
162 lands. 'Peatland' in CESM2 refers to soils with high organic matter content, and its areal
163 coverage is derived from a combination of geologic surveys and global databases (Lawrence
164 et al., 2018; Tarnocai et al., 2011; Wells et al., 2010). Peatland cover is a prescribed char-
165 acteristic of the land model.

166 **3 Results**

167 **3.1 Permafrost and related fields**

168 We begin by comparing the time series of terrestrial permafrost extent north of 50°N
169 in the SSP2-4.5 (control) and ARISE-SAI-1.5 simulations (Fig. 1a). In the control sim-

170 ulations (red dashed line), the ensemble mean permafrost extent steadily declines at an
 171 average rate of 0.08 million km² year⁻¹. In the ARISE-SAI-1.5 simulations, the ensem-
 172 ble mean permafrost extent (blue solid line) declines at a rate of 0.04 million km² year⁻¹
 173 from 2035–2045. The rate of thaw starts to slow down over time, but does not completely
 174 stabilize. For the last 10 years of the simulation, 2060–2069, permafrost extent under SAI
 175 declines at a rate of 0.02 million km² year⁻¹. Along with smaller permafrost extent, there
 176 is also less permafrost by volume from 2015–2069 in SSP2-4.5 (Fig. 1b). Unlike the de-
 177 cline in extent, however, permafrost volume does not shrink at a constant rate, and ac-
 178 tually remains at roughly 33.5 km³ for the last decade of the simulation. Under SAI (blue
 179 solid line), the ensemble mean permafrost volume only decreases by 0.6 km³ from 2035–
 180 2069, and half of that volume loss occurs before 2042. For both simulations there is a
 181 lot more interannual variability in volume than in extent. The annual mean SSP2-4.5
 182 temperature increases by ~1°C from 2015–2069, but stays near -4°C for the last decade
 183 (Fig. 1c). The ARISE-SAI-1.5 ensemble mean temperature gets slightly colder over the
 184 simulation, and is 1.2°C colder than the SSP2-4.5 ensemble mean temperature by 2069.

185 While the total permafrost extent continues to decline under both simulations (Fig.
 186 1a), changes to the active layer depth (Fig. 2) indicate that SAI does have a noticeable
 187 influence on permafrost. As expected, ALTMAX is deepest (> 3 m) at the lowest lat-
 188 itude of permafrost extent, where permafrost is warmest and most degraded, during 2035–
 189 2044 in SSP2-4.5 (Fig. 2a) and ARISE-SAI-1.5 (Fig. 2b). By 2060–2069, ALTMAX is
 190 still > 3 m along much of the permafrost area margin, but is generally deeper in SSP2-
 191 4.5 (Fig. 2c) compared with ARISE-SAI-1.5 (Fig. 2d). SAI's effect on the active layer
 192 is most apparent when looking at the differences in ALTMAX between 2035–2044 and
 193 2060–2069 in the two simulations (Fig. 2e, 2f). ALTMAX increases by up to 30 cm in
 194 most of Canada and northern Russia in SSP2-4.5, but also decreases by 5–25 cm in parts
 195 of southern Russia (Fig. 2e).

196 Even though total permafrost extent does not fully stabilize or recover by 2069 un-
 197 der SAI (Fig. 1a), active layer depth remains stable in most of the permafrost region in
 198 ARISE-SAI-1.5 (white cells in Fig. 2f). Furthermore, there are some places where new
 199 permafrost forms between 2035–2044 and 2060–2069 (green cells in Fig. 2f). New per-
 200 mafrost may form either because soil in a previously thawed grid cell permanently freezes,
 201 or because the ALTMAX in that grid cell becomes shallower than the bedrock depth.
 202 The black cells denote the presence of an active layer in the SSP2-4.5 or ARISE-SAI-

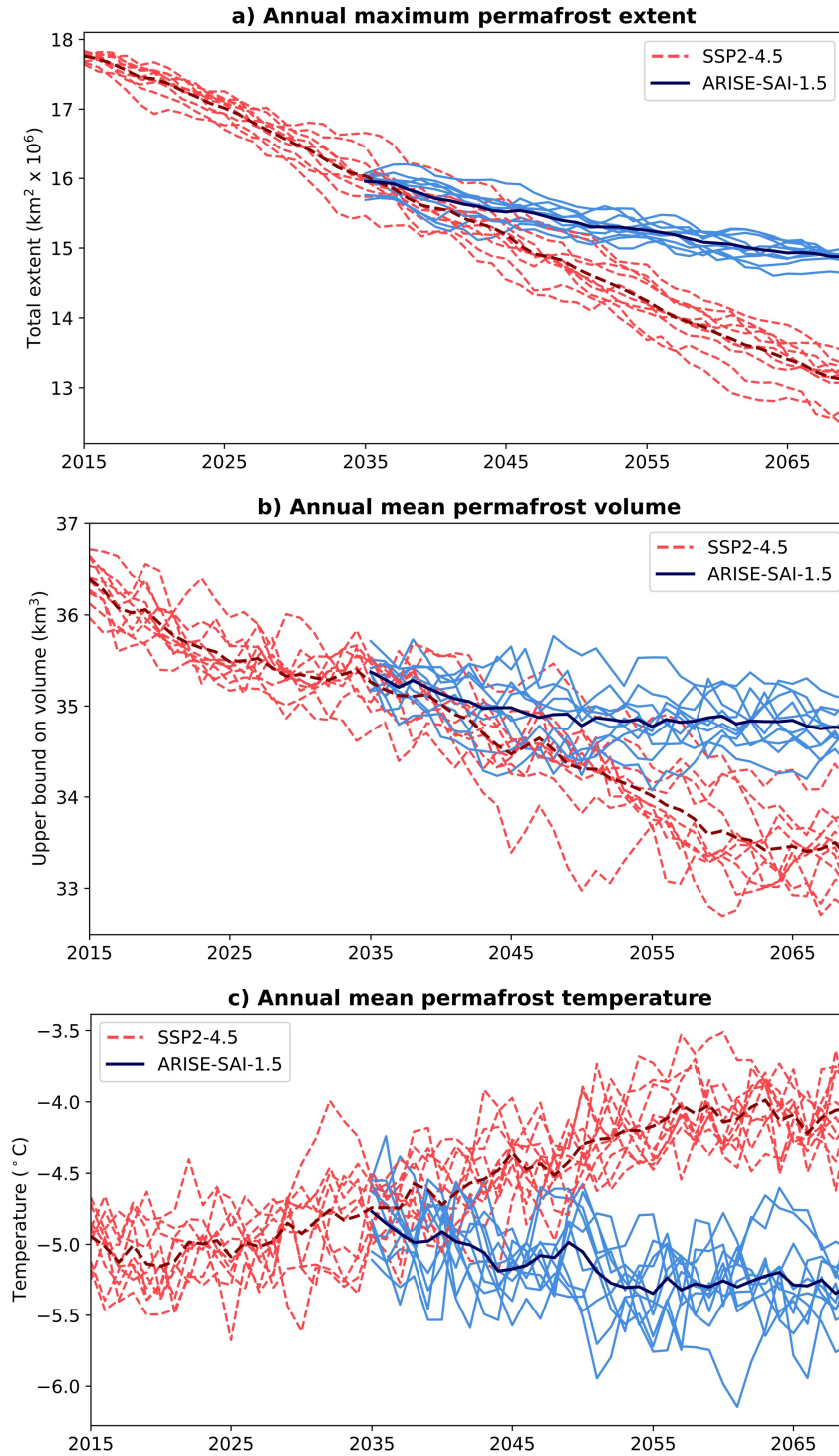


Figure 1. Time series of annual a) maximum permafrost extent, b) mean permafrost volume, and c) mean permafrost temperature for the SSP2-4.5 (red dashed line) and ARISE-SAI-1.5 (blue solid line) simulations. All time series are over land north of 50°N. Thin lines are individual ensemble members; thick lines are the ensemble means.

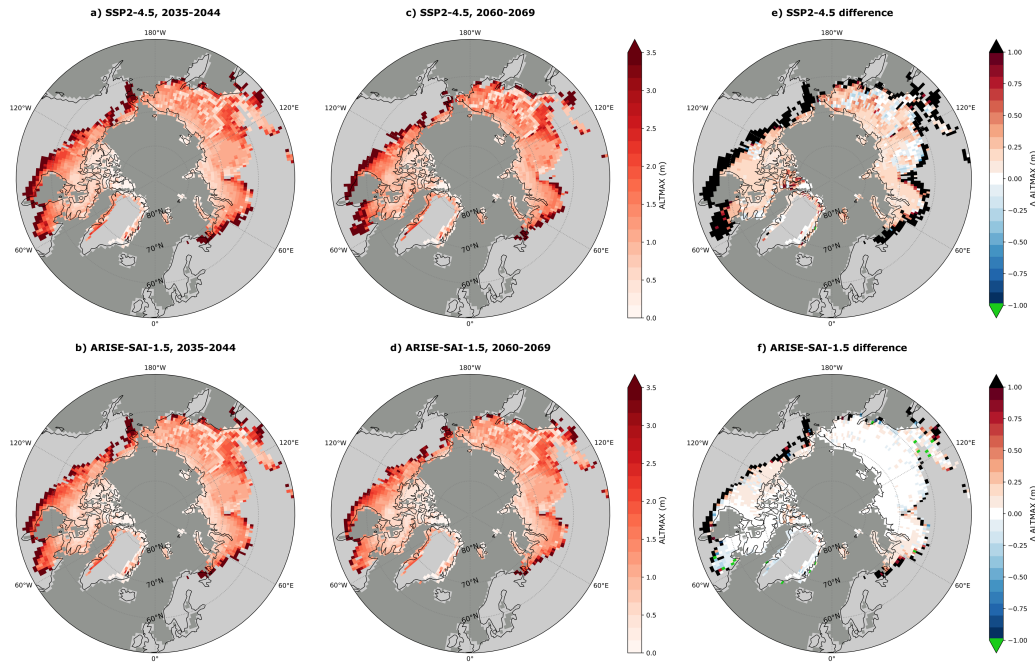


Figure 2. Annual maximum active layer depth (ALTMAX) in the ensemble mean a) SSP2-4.5 and b) ARISE-SAI-1.5 simulations from 2035–2044 and c) SSP2-4.5 and d) ARISE-SAI-1.5 simulations from 2060–2069. Difference in ALTMAX in the ensemble mean e) SSP2-4.5 and f) ARISE-SAI-1.5 simulations, 2060–2069 minus 2035–2044. Black cells are where permafrost exists in 2035–2044 but has thawed by 2060–2069. Green cells are where permafrost has frozen by 2060–2069 but did not exist in 2035–2044.

203 1.5 ensemble mean from 2035–2044 but not from 2060–2069. That is, the black cells along
 204 the southernmost margin of the permafrost region are where permafrost exists at the be-
 205 ginning of the simulations but then thaws and disappears by the end, or where ALTMAX
 206 becomes deeper than the bedrock depth.

207 3.2 Critical climate conditions for permafrost

208 Just as SAI prevents the annual maximum active layer depth from getting deeper
 209 in much of the permafrost region (Fig. 2f), it also delays or prevents most projected talik
 210 formation. Color shading in Figure 3a and 3b indicates the first year that talik forms
 211 in each simulation ensemble mean, and the green line denotes cells that contain >10%
 212 peatland in CESM2. SSP2-4.5 projects widespread talik formation across northern Canada
 213 and Alaska, starting in the lower latitudes in 2015 and moving poleward through 2069

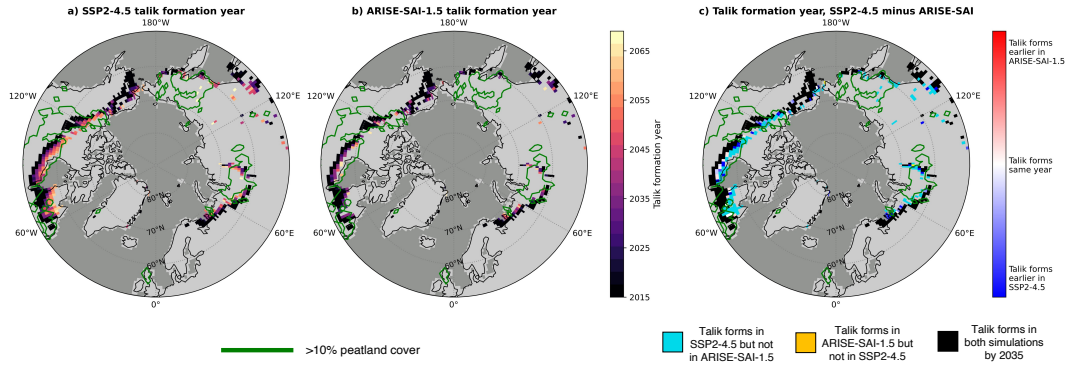


Figure 3. First year of projected talik formation in a) SSP2-4.5 and b) ARISE-SAI-1.5 ensemble mean simulations. Green line indicates where land is >10% peatland in CESM2 based on organic matter content. c) Difference in year of projected talik formation, SSP2-4.5 minus ARISE-SAI-1.5 ensemble means. Dark blue cells are where talik forms earlier in SSP2-4.5 than in ARISE-SAI-1.5, red cells are where talik forms earlier in ARISE-SAI-1.5 than in SSP2-4.5, cyan cells are where talik forms in SSP2-4.5 by 2069 but does *not* form in ARISE-SAI-1.5, yellow cells are where talik forms in ARISE-SAI-1.5 by 2069 but does *not* form in SSP2-4.5, and black cells are where talik has formed in both simulations by 2035.

214 (Fig. 3a). Less talik forms in ARISE-SAI-1.5 (Fig. 3b), and much of the talik that is pro-
 215 jected to exist in this simulation has already formed by 2035 (black cells in Fig. 3a, 3b),
 216 or by the beginning of SAI deployment. Note that the cells with the most permafrost
 217 thaw (black cells in Fig. 2e, 2f) had already formed talik when SAI started in 2035. SAI
 218 prevents talik formation in 1.1 million km² of permafrost compared with SSP2-4.5 (cyan
 219 cells in Fig. 3c; Fig. 4) and delays talik formation by up to 20 years in 0.3 million km²
 220 of permafrost (dark blue cells in Fig. 3c). Roughly 64% of the talik formation that is
 221 either delayed or prevented by SAI is in peatland (green line in Fig. 3). The area of per-
 222 mafrost that contains talik in SSP2-4.5 rises at a fairly constant rate, increasing by 168%
 223 in the ensemble mean from 2015–2069, and by 68% from 2035–2069. From 2035–2069,
 224 the area containing talik in the ARISE-SAI-1.5 ensemble mean increases by only 18%
 225 (Fig. 4).

226 Much of the talik formation prevented by SAI is in peatlands, but how much to-
 227 tal permafrost peatland thaw could SAI prevent in this scenario? In CESM2, the largest
 228 peatland cover poleward of 50°N is found in Canada along the coast of Hudson Bay (Fig.

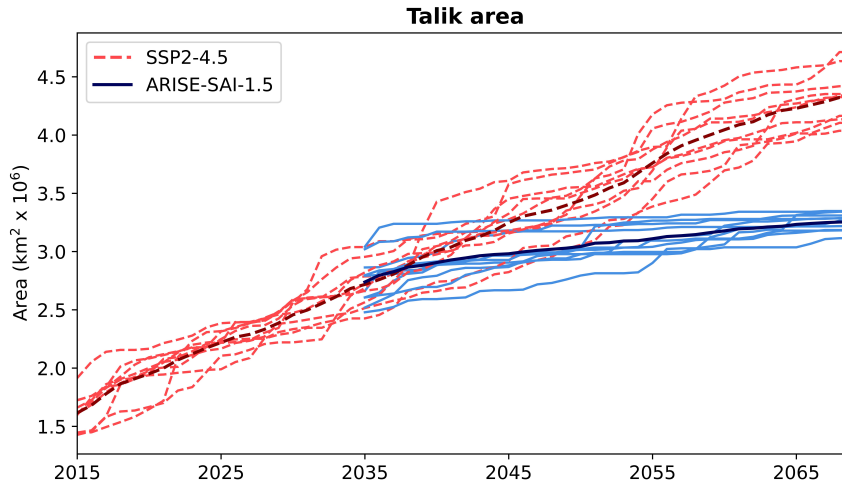


Figure 4. Total area of grid cells that contain talik in the SSP2-4.5 (red dashed line) and ARISE-SAI-1.5 (blue solid line) simulations. Thin lines are individual ensemble members; thick lines are the ensemble means.

229 5a). Figure 5b shows the time series of the percentage of permafrost peatland remain-
 230 ing relative to 2035 values in SSP2-4.5 (red dashed lines) and ARISE-SAI-1.5 (blue solid
 231 lines). Permafrost peatland is only considered in grid cells with >10% peatland cover
 232 (see green line in Fig. 3). Permafrost peatland area declines in both simulations, but de-
 233 creases at a nearly linear rate in SSP2-4.5 compared with a more gradual decline in ARISE-
 234 SAI-1.5. By 2045, significantly more permafrost peatland remains in ARISE-SAI-1.5 com-
 235 pared with SSP2-4.5 ($p < 0.05$). By 2069, ~70% of total permafrost peatland remains
 236 in the SSP2-4.5 ensemble mean, compared with ~92% remaining in the ARISE-SAI-1.5
 237 ensemble mean.

238 Identifying SAI's influence on permafrost is not only important for understanding
 239 the physical changes to permafrost but also for the downstream effects of permafrost thaw,
 240 which includes changes to carbon stocks. Figure 6 shows changes in total ecosystem car-
 241 bon (ΔECOC) per unit area from 2035–2069 from the entire permafrost region (Fig. 6a)
 242 and from only permafrost peatland (Fig. 6b). Again, permafrost peatland is only con-
 243 sidered in grid cells with >10% peatland cover. As discussed in section 2.2, ΔECOC is
 244 given in per unit area to account for the difference in permafrost area between the sim-
 245 ulations and the year-to-year differences in permafrost area within each simulation. Un-

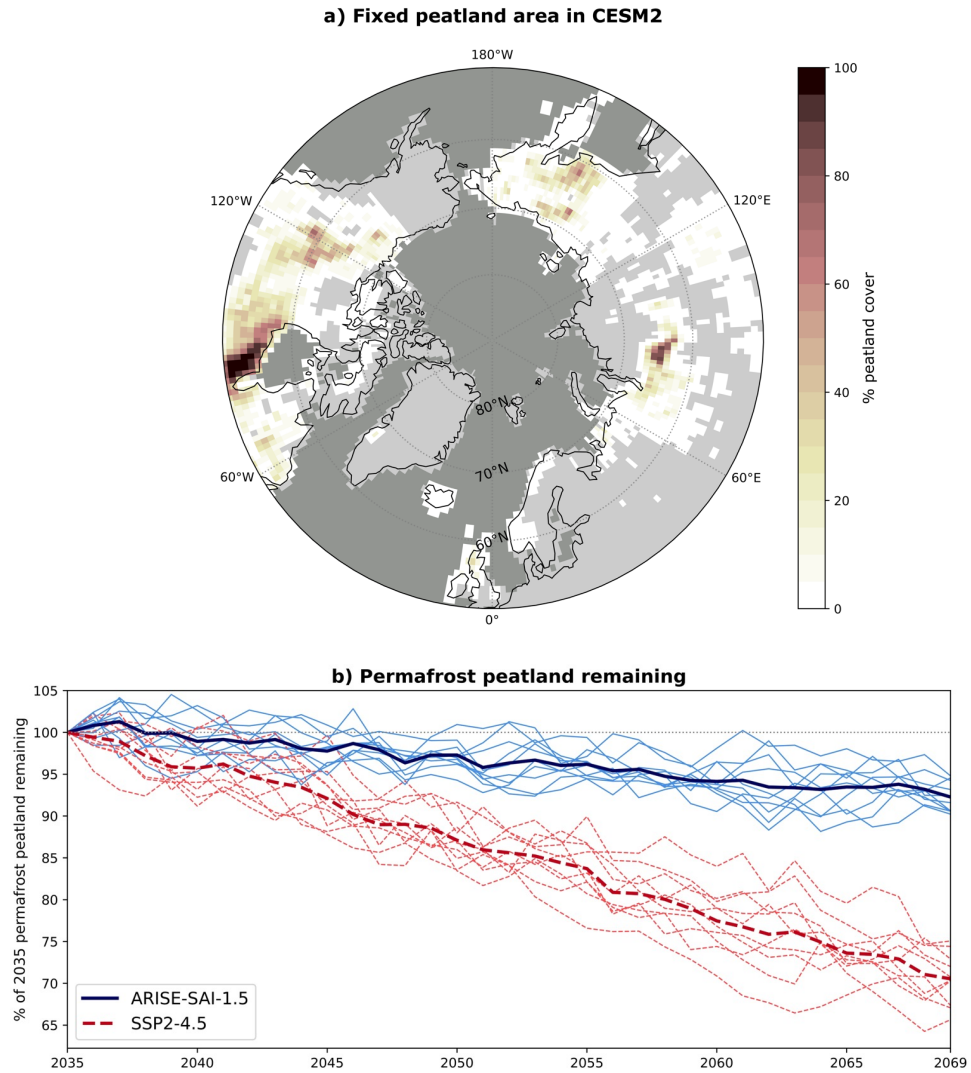


Figure 5. a) Prescribed peatland cover in CESM2 based on soil organic matter content. Peatland cover is a fixed constant in CESM2. b) Percent of 2035 annual mean permafrost soil in grid cells with $>10\%$ peatland cover in SSP2-4.5 (red dashed line) and ARISE-SAI-1.5 (blue solid line) simulations. Thin lines are individual ensemble members; thick lines are the ensemble means.

246 der SSP2-4.5, land carbon stocks in the total permafrost and permafrost peatland re-
247 gions increase, while permafrost carbon under SAI remains nearly constant (Fig. 6a).

248 Why does ΔECOC increase in SSP2-4.5 but stay close to zero in ARISE-SAI-1.5?
249 As the Arctic warms under SSP2-4.5, CO_2 concentrations increase, and the environment
250 becomes more conducive to plant growth which adds more carbon back into the system
251 via photosynthesis and increased root litter. Permafrost thaw still leads to enhanced mi-
252 crobial activity in the thawed soil and more carbon release through respiration and de-
253 composition, but enhanced vegetation puts more carbon into the permafrost environment
254 than microbial activity removes. Until 2045, the permafrost carbon sinks and sources
255 in ARISE-SAI-1.5 are well-balanced, leading to a near-zero ΔECOC . As surface tem-
256 peratures stabilize under SAI and the rate of permafrost thaw begins to slow down, how-
257 ever, plant growth in response to increasing CO_2 concentrations begins to outweigh the
258 loss of carbon through respiration and decomposition. As a result, ΔECOC under SAI
259 becomes slightly positive over time.

260 4 Discussion

261 One key result of our study is that total permafrost extent still declines (Fig. 1a)
262 and some permafrost thaws completely (Fig. 2f) under the ARISE-SAI-1.5 scenario. The
263 permafrost that completely thaws in both simulations is at the lowest latitude of per-
264 mafrost extent and is vulnerable to thaw because it is greater than 3 m underground at
265 the start of the stratospheric aerosol deployment in 2035 (Fig. 2a, 2b). Permafrost un-
266 der a deep active layer is warmer than near-surface permafrost, and therefore more likely
267 to imminently thaw. Deeper permafrost is also resistant to changes in surface temper-
268 atures and precipitation. The low latitude permafrost that thaws in SSP2-4.5 but does
269 not thaw in ARISE-SAI-1.5, mostly located in southern Russia, is under a shallower ac-
270 tive layer and may respond faster to surface temperature changes. Furthermore, most
271 of the ‘vulnerable’ permafrost that thaws in both simulations already contained talik by
272 the time SAI was deployed (Fig. 3b). That is, most of the degraded permafrost had al-
273 ready reached a critical condition for rapid thaw (i.e., a tipping point) that SAI could
274 not prevent in the ARISE-SAI-1.5 simulations. Shallow talik can potentially re-freeze
275 in the winter if temperatures are cold enough and there is sparse snow cover (Farquharson
276 et al., 2022; Fewster et al., 2022). SAI is successful at preventing permafrost tipping points
277 in the permafrost that can be preserved – that is, thaw and talik formation are still pre-

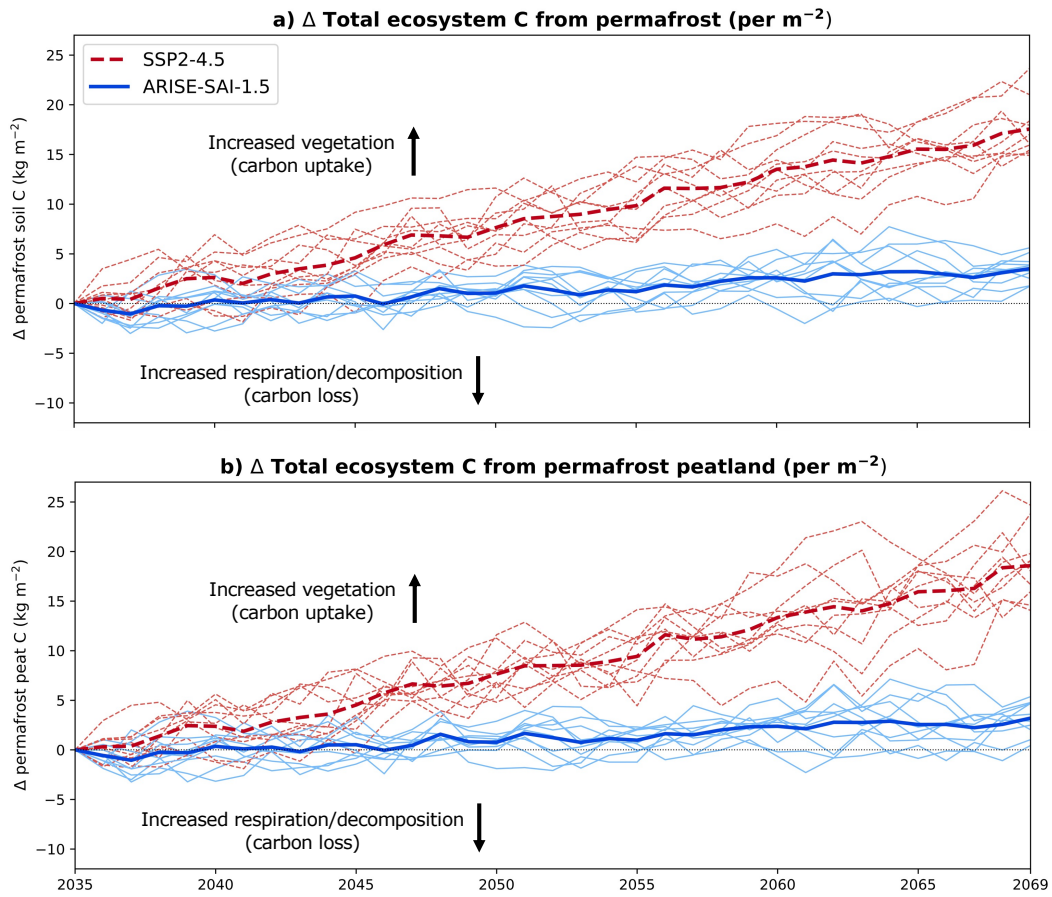


Figure 6. Change in annual mean total ecosystem carbon (ΔECOC) per unit area in a) total permafrost and b) permafrost grid cells that are $>10\%$ peatland from 2035–2069 in the SSP2-4.5 (red dashed lines) and ARISE-SAI-1.5 (blue solid lines) simulations. Thin lines are individual ensemble members; thick lines are the ensemble means. Positive (negative) ΔECOC indicates that increased vegetation carbon offsets (is outweighed by) increased soil carbon loss through respiration and decomposition.

278 vented in the cold shallow permafrost that is responsive to the temperature changes that
279 SAI produces. Another tipping point potentially avoided by SAI is the irreversible loss
280 of carbon from peatlands. For example, carbon stocks on coastal Hudson Bay are likely
281 irrecoverable if released into the atmosphere (Noon et al., 2022), and ARISE-SAI-1.5 pre-
282 serves more than 90% of the permafrost in this region (Fig. 5b).

283 Despite steadily thawing permafrost (Fig. 1, Fig. 2) and talik formation across an
284 increasing area (Fig. 3a, Fig. 4), the permafrost region in SSP2-4.5 continues to be a car-
285 bon sink through 2069 (Fig. 6). Under most plausible climate trajectories, permafrost
286 soils are projected to switch from a carbon sink to a carbon source as continued warm-
287 ing thaws permafrost and increases the depth of soil available for microbial activity (e.g.,
288 Koven et al., 2015; McGuire et al., 2018; Parazoo et al., 2018; Schuur et al., 2008). Talik
289 formation can also trigger a transition from carbon sink to source. The timing of the sink-
290 to-source transition is regionally variable, but in many areas occurs after 2070, or after
291 the end of the simulations assessed in this study (Parazoo et al., 2018). From 2035–2069,
292 the positive ΔECOC under SSP2-4.5 captures projected increases in soil carbon asso-
293 ciated with enhanced vegetation productivity and increased plant litter. It also indicates
294 that permafrost does not thaw enough under SSP2-4.5 from 2035–2069 to offset ecosys-
295 tem carbon gains from vegetation changes. Increased plant cover, especially shrubs, has
296 also been correlated with reduced summer permafrost thaw by reducing the amount of
297 sunlight that reaches the ground surface (Blok et al., 2010). Warmer temperatures could
298 also lengthen the growing season, giving plants more time to sequester carbon. These
299 vegetation changes may make the permafrost region a stronger (short term) carbon sink
300 in SSP2-4.5 than under ARISE-SAI-1.5.

301 Over the same time period in ARISE-SAI-1.5 there is only a small increase in ΔECOC
302 (Fig. 6). The small increase indicates that the balance between net ecosystem carbon
303 loss and net ecosystem carbon gain is slightly tipped in favor of net carbon gain, but not
304 as much as it is in SSP2-4.5. Even without warmer temperatures, the tundra may be-
305 come more productive under SAI as CO_2 -driven plant growth responds to increasing CO_2
306 concentrations. As in SSP2-4.5, increased plant cover could reduce potential summer per-
307 mafrost thaw, but the shading influence may be reduced because aerosols are already block-
308 ing some incoming sunlight. In both a potential SAI and non-SAI world there is an up-
309 per bound on how hospitable the permafrost region can be to new vegetation because
310 of sunlight, nutrient, and temperature limitations (Mekonnen et al., 2021; Riley et al.,

2021; Zhang et al., 2022). Eventually carbon uptake may stagnate and no longer offset
carbon losses from increased warming and permafrost thaw. Those timescales, however,
are outside the current scope of these simulations. In the short term, permafrost soils
under SSP2-4.5 sequester more carbon than permafrost soils under SAI.

There are a few caveats to our study that should be kept in mind. For instance,
some permafrost processes are not fully represented in the current generation of Earth
system models. Processes such as thaw-induced slumps or thermokarst production oc-
cur at resolutions too fine to be captured in the CESM2 model, both of which can rapidly
release carbon that the model may not capture. Processes related to talik formation are
also difficult to implement. Taliks often form beneath lakes or rivers that are not resolved
in most Earth system models. As a result, our projections may underestimate how much
talik forms in both the SSP2-4.5 and ARISE-SAI-1.5 simulations. We also define talik
solely by temperature from Parazoo et al. (2018), but do not account for small-scale soil
hydrology characteristics that affect talik formation (Treat et al., 2022). Our findings
do agree with studies that observed degraded permafrost and talik at sites in Alaska (Farquharson
et al., 2022) and the Northwest Territories (Connon et al., 2018) before 2020, in regions
where talik is projected to form before 2020 in SSP2-4.5 (Fig. 3a).

Our results generally agree with previous studies that find that different SAI pro-
tocols can reduce permafrost thaw and permafrost temperature relative to a non-SAI world
(Chen et al., 2020, 2023; H. Lee et al., 2019; W. Lee et al., 2023). While preserving some
low latitude permafrost through ARISE-SAI-1.5 may be impossible, it remains to be seen
whether climate intervention strategies with more aggressive temperature targets (e.g.,
to limit warming to 0.5°C or 1°C) or earlier deployment may be sufficient to better pre-
vent permafrost thaw. SAI with region-specific goals has been shown to increase permafrost
area (W. Lee et al., 2023). It is important to note, however, that different SAI strate-
gies may come with their own suite of potential side effects (Tang & Kemp, 2021).

5 Conclusions

We assessed the possible influence of SAI on Northern Hemisphere terrestrial per-
mafrost, with a particular interest in whether the SAI as deployed in the ARISE-SAI-
1.5 simulations could prevent tipping points that lead to accelerated permafrost thaw.
Using a variable bedrock depth to restrict permafrost only to the land model's soil lay-

ers restricts our analysis only to potentially biogeochemically active permafrost. While permafrost extent continues to decline under SAI, this is due to deeper permafrost disappearing along the southern margin of the permafrost region. Talik had already formed within this vulnerable region when SAI was deployed in the model, potentially tipping these permafrost cells into a critical climate condition where the entire soil column thaws down to the bedrock. Outside of this deeper permafrost, the active layer stabilizes in ARISE-SAI-1.5, and even new permafrost forms in parts of southern Russia. Most of the talik formation projected to occur in the SSP2-4.5 simulations is delayed or prevented entirely by SAI. Preventing permafrost thaw also leads to a small increase in total ecosystem carbon, likely due to enhanced productivity, but this carbon increase is smaller under SAI than under SSP2-4.5 conditions. Our results suggest that while SAI - as simulated by ARISE-SAI-1.5 - may be effective in stabilizing active layer depth and preventing talik formation outside of the most vulnerable permafrost regions, more aggressive SAI strategies with lower temperature targets may be required to stop ongoing and future permafrost thaw or significantly reduce the carbon released from thawing permafrost soils.

6 Open Research

All Python code and processed data for this analysis are available at https://github.com/eabarnes1010/actm-sai-csu/tree/main/research/arise_arctic_climate. At the time of publication this will be converted to a permanent repository on Zenodo. The unprocessed monthly mean ARISE-SAI-1.5 and SSP2-4.5 data that support this study are publicly available from Richter (2022) and Mills et al. (2022), respectively.

Acknowledgments

This work was supported by Defense Advanced Research Projects Agency (DARPA) Grant No. HR00112290071. The views expressed here do not necessarily reflect the positions of the U.S. government. We would like to acknowledge high-performance computing support from Cheyenne (doi:10.5065/D6RX99HX) provided by NCAR's Computational and Information Systems Laboratory, sponsored by the National Science Foundation. A.L.M. and J.W.H. were also supported by the LAD climate group. We declare no competing interests.

371 **References**

- 372 Armstrong McKay, D. I., Staal, A., Abrams, J. F., Winkelmann, R., Sakschewski,
 373 B., Loriani, S., ... Lenton, T. M. (2022). Exceeding 1.5°C global warm-
 374 ing could trigger multiple tipping points. *Science*, *377*, eabn7950. doi:
 375 10.1126/science.abn7950
- 376 Blok, D., Heijmans, M. M. P. D., Schaepman-Strub, G., Kononov, A. V., Maximov,
 377 T. C., & Berendse, F. (2010). Shrub expansion may reduce summer per-
 378 mafrost thaw in siberian tundra. *Global Change Biology*, *16*(4), 1296–1305.
 379 doi: 10.1111/j.1365-2486.2009.02110.x
- 380 Chen, Y., Ji, D., Zhang, Q., Moore, J. C., Boucher, O., Jones, A., ... Tilmes, S.
 381 (2023). Northern-high-latitude permafrost and terrestrial carbon response to
 382 two solar geoengineering scenarios. *Earth System Dynamics*, *14*, 55–79. doi:
 383 doi.org/10.5194/esd-14-55-2023
- 384 Chen, Y., Liu, A., & Moore, J. C. (2020). Mitigation of arctic permafrost carbon
 385 loss through stratospheric aerosol geoengineering. *Nature Communications*,
 386 *11*(2430). doi: doi.org/10.1038/s41467-020-16357-8
- 387 Connon, R. F., Devoie, E. G., Hayashi, M., Veness, T., & Quinton, Q. (2018). The
 388 influence of shallow taliks on permafrost thaw and active layer dynamics in
 389 subarctic canada. *Journal of Geophysical Research: Earth Surface*, *123*(2),
 390 281–297. doi: doi.org/10.1002/2017JF004469
- 391 Dagon, K., & Schrag, D. P. (2017). Regional climate variability under model simu-
 392 lations of solar geoengineering. *Journal of Geophysical Research: Atmospheres*,
 393 *122*(22), 12106–12121. doi: 10.1002/2017JD027110
- 394 Danabasoglu, G., Lamarque, J.-F., Bacmeister, J., Bailey, D. A., DuVivier, A. K.,
 395 Edwards, J., ... Strand, W. G. (2020). The community earth system model
 396 version 2 (cesm2). *Journal of Advances in Modeling Earth Systems*, *12*(2),
 397 e2019MS001916. doi: doi.org/10.1029/2019MS001916
- 398 Devoie, E. G., Craig, J. R., Connon, R. F., & Quinton, W. L. (2019). Taliks: A
 399 tipping point in discontinuous permafrost degradation in peatlands. *Water Re-*
 400 *sources Research*, *55*, 9839–9857. doi: 10.1029/2018WR024488
- 401 Farquharson, L. M., Romanovsky, V. E., Kholodov, A., & Nicolsky, D. (2022). Sub-
 402 aerial talik formation observed across the discontinuous permafrost zone of
 403 alaska. *Nature Geoscience*, *15*, 475–481.

- 404 Fewster, R. E., Morris, P. J., Ivanovic, R. F., Swindles, G. T., Peregon, A. M., &
 405 Smith, C. J. (2022). Imminent loss of climate space for permafrost peatlands
 406 in europe and western siberia. *Nature Climate Change*, *12*, 373–379.
- 407 Gettelman, A., Mills, M. J., Kinnison, D., Garcia, R., Smith, A., Marsh, D., ...
 408 Randel, J. (2019). The whole atmosphere community climate model ver-
 409 sion 6 (waccm6). *Journal of Geophysical Research: Atmospheres*, *124*(23),
 410 12380–12403. doi: doi.org/10.1029/2019JD030943
- 411 Heffernan, L., Estop-Aragónés, C., Knorr, K.-H., Talbot, J., & Olefeldt, D. (2020).
 412 Long-term impacts of permafrost thaw on carbon storage in peatlands: Deep
 413 losses offset by surficial accumulation. *Journal of Geophysical Research: Bio-*
 414 *geosciences*, *125*, e2019JG005501. doi: doi.org/10.1029/2019JG005501
- 415 Hugelius, G., Loisel, J., Chadburn, S., Jackson, R. B., Jones, M., MacDonald,
 416 G., ... Yu, Z. (2020). Large stocks of peatland carbon and nitrogen
 417 are vulnerable to permafrost thaw. *PNAS*, *117*(34), 20438–20446. doi:
 418 doi:10.1073/pnas.1916387117
- 419 Hugelius, G., Strauss, J., Zubrzycki, S., Harde, J. W., Schuur, E. A. G., Ping, C.-L.,
 420 ... Kuhry, P. (2014). Estimated stocks of circumpolar permafrost carbon with
 421 quantified uncertainty ranges and identified data gaps. *Biogeosciences*, *11*,
 422 6573–6593. doi: 10.5194/bg-11-6573-2014
- 423 Jones, M., Harden, J., O'Donnell, J., Manies, K., Jorgenson, T., Treat, C., & Ewing,
 424 S. (2016). Rapid carbon loss and slow recovery following permafrost thaw in
 425 boreal peatlands. *Global Change Biology*, *23*(3), 1109–1127.
- 426 Keith, D. (2000). Geoengineering the climate: History and prospect. *Annual Review*
 427 *of Energy and the Environment*, *25*, 245–284. doi: 10.1146/annurev.energy.25
 428 .1.245
- 429 Könönen, O. H., Karjalainen, O., Aalto, J., Luoto, M., & Hjort, J. (2023). Environ-
 430 mental spaces for palsas and peat plateaus are disappearing at a circumpolar
 431 scale. *The Cryosphere*. doi: doi.org/10.5194/tc-2022-135
- 432 Koven, C., Lawrence, D., & Riley, W. (2015). Permafrost carbonclimate feedback
 433 is sensitive to deep soil carbon decomposability but not deep soil nitrogen
 434 dynamics. *Proc. Natl. Acad. Sci. U.S.A.*, *112*(12), 3752–3757.
- 435 Kravitz, B., MacMartin, D. G., Mills, M. J., Richter, J. H., Tilmes, S., Lamarque,
 436 J.-F., ... Vitt, F. (2017). First simulations of designing stratospheric sul-

- 437 fate aerosol geoengineering to meet multiple simultaneous climate objectives.
 438 *Journal of Geophysical Research: Atmospheres*, *122*(23), 12616–12634.
- 439 Lawrence, D., Fisher, R., Koven, C., Oleson, K., Swenson, S., Bonan, G., . . . Zeng,
 440 X. (2019). The community land model version 5: Description of new features,
 441 benchmarking, and impact of forcing uncertainty. *Journal of Advances in*
 442 *Modeling Earth Systems*, *11*, 4245–4287.
- 443 Lawrence, D., Fisher, R., Koven, C., Oleson, K., Swenson, S., Vertenstein, M., . . .
 444 Zeng, X. (2018). *Technical description of version 5.0 of the community land*
 445 *model (clm)* [report]. National Center for Atmospheric Research, Boulder,
 446 CO. Retrieved from [https://www2.cesm.ucar.edu/models/cesm2/land/](https://www2.cesm.ucar.edu/models/cesm2/land/CLM50_Tech_Note.pdf)
 447 [CLM50_Tech_Note.pdf](https://www2.cesm.ucar.edu/models/cesm2/land/CLM50_Tech_Note.pdf)
- 448 Lee, H., Altug, E., Tjiputra, J., Muri, H., Chadburn, S. E., Lawrence, D. M., &
 449 Schwinger, J. (2019). The response of permafrost and high-latitude ecosystems
 450 under large-scale stratospheric aerosol injection and its termination. *Earth's*
 451 *Future*, *7*(6), 605–614. doi: 10.1029/2018EF001146
- 452 Lee, W., MacMartin, D. G., Vioni, D., Kravitz, B., Chen, Y., Moore, J. C., . . .
 453 Bailey, D. A. (2023). High-latitude stratospheric aerosol injection to pre-
 454 serve the arctic. *Earth's Future*, *11*, e2022EF003052. doi: doi.org/10.1029/
 455 2022EF003052
- 456 Lenton, T. (2012). Arctic climate tipping points. *AMBIO*, *41*, 10–22.
- 457 Liu, A., Moore, J. C., & Chen, Y. (2023). Pinc-panther estimates of arctic per-
 458 mafrost soil carbon under the geomip g6solar and g6sulfur experiments. *Earth*
 459 *System Dynamics*, *14*, 39–53. doi: doi.org/10.5194/esd-14-39-2023
- 460 MacMartin, D. G., Kravitz, B., Keith, D. W., & Jarvis, A. (2014). Dynamics of
 461 the coupled human–climate system resulting from closed-loop control of solar
 462 geoengineering. *Climate Dynamics*, *43*, 243–258.
- 463 Manies, K. L., Jones, M. C., Waldrop, M. P., Leewis, M.-C., Fuller, C., Cornman,
 464 R. S., & Hoekfe, K. (2021). Influence of permafrost type and site history
 465 on losses of permafrost carbon after thaw. *Journal of Geophysical Research:*
 466 *Biogeosciences*, *126*, e2021JG006396.
- 467 McGuire, A. D., Lawrence, D. M., Koven, C., Klein, J. S., Burke, E., Chen, G.,
 468 . . . Zhuang, Q. (2018). Dependence of the evolution of carbon dynamics in
 469 thenorthern permafrost region on the trajectory of climate change. *PNAS*,

- 470 115(5), 3882–3887.
- 471 Mekonnen, Z. A., Riley, W. J., Berner, L. T., Bouskill, N. J., Torn, M. S., Iwahana,
472 G., ... Liu, Y. (2021). Arctic tundra shrubification: a review of mechanisms
473 and impacts on ecosystem carbon balance. *Environmental Research Letters*,
474 16, 053001. doi: 10.1088/1748-9326/abf28b
- 475 Mills, M., Vioni, D., & Richter, J. H. (2022). *Cesm2 model output cesm2-waccm6-*
476 *ssp245* [dataset]. NCAR. Retrieved from [https://www.earthsystemgrid](https://www.earthsystemgrid.org/dataset/ucar.cgd.cesm2.waccm6.ssp245.html)
477 [.org/dataset/ucar.cgd.cesm2.waccm6.ssp245.html](https://www.earthsystemgrid.org/dataset/ucar.cgd.cesm2.waccm6.ssp245.html) doi: 10.26024/
478 0cs0-ev98
- 479 Noon, M. L., Goldstein, A., Ledezma, J. C., Roehrdanz, P. R., Cook-Patton, S. C.,
480 Spawn-Lee, S. A., ... Turner, W. R. (2022). Mapping the irrecoverable carbon
481 in earth's ecosystems. *Nature Sustainability*, 5, 37–46.
- 482 Parazoo, N. C., Koven, C. D., Lawrence, D. M., Romanovsky, V., & Miller, C. E.
483 (2018). Detecting the permafrost carbon feedback: talik formation and in-
484 creased cold-season respiration as precursors to sink-to-source transitions. *The*
485 *Cryosphere*, 12, 123–144. doi: 10.5194/tc-12-123-2018
- 486 Pihl, E., Martin, M. A., Blome, T., Hebden, S., Jarzebski, M. P., Lambino, R. A.,
487 ... Sonntag, S. (2019). *10 new insights in climate science 2019*. Stockholm:
488 Future Earth & The Earth League.
- 489 Rantanen, M., Karpechko, A. Y., Lipponen, A., Nordling, K., Hyvärinen, O., Ru-
490 osteenoja, K., ... Laaksonen, A. (2022). The arctic has warmed nearly four
491 times faster than the globe since 1979. *Communications Earth Environment*,
492 3(168), 4007–4037. doi: doi.org/10.1038/s43247-022-00498-3
- 493 Rasch, P. J., Tilmes, S., Turco, R. P., Robock, A., Oman, L., Chen, C.-C., ... Gar-
494 cia, R. R. (2008). An overview of geoengineering of climate using stratospheric
495 sulphate aerosols. *Philosophical Transactions of the Royal Society A*, 366,
496 4007–4037. doi: doi:10.1098/rsta.2008.0131
- 497 Riahi, K., van Vuuren, D. P., Kriegler, E., Edmonds, J., O'Neill, B., Fujimori, S.,
498 ... Tavoni, M. (2017). The shared socioeconomic pathways and their energy,
499 land use, and greenhouse gas emissions implications: An overview. *Global*
500 *Environmental Change*, 42, 153–168. doi: 10.1016/j.gloenvcha.2016.05.009
- 501 Richter, J. H. (2022). *Cesm2 model output arise-sai-1.5 dataset* [dataset].
502 NCAR. Retrieved from <https://www.earthsystemgrid.org/dataset/>

- 503 ucar.cgd.cesm4.ARISE-SAI-1.5.html doi: 10.5065/9kcn-9y79
- 504 Richter, J. H., Vioni, D., MacMartin, D. G., Bailey, D. A., Rosenbloom, N., Dob-
505 bins, B., . . . Lamarque, J.-F. (2022). Assessing responses and impacts of solar
506 climate intervention on the earth system with stratospheric aerosol injection
507 (arise-sai): protocol and initial results from the first simulations. *Geoscientific*
508 *Model Development*, 15, 8221-8243. doi: 10.5194/gmd-15-8221-2022
- 509 Riley, W. J., Mekonnen, Z. A., Tang, J., Zhu, Q., , Bouskill, N. J., & Grant, R. F.
510 (2021). Non-growing season plant nutrient uptake controls arctic tundra vege-
511 tation composition under future climate. *Environmental Research Letters*, 16,
512 074047. doi: 10.1088/1748-9326/ac0e63
- 513 Schuur, E. A. G., Bockheim, J., Canadell, J. G., Euskirchen, E., Field, C. B., Gory-
514 achkin, S. V., . . . Zimov, S. A. (2008). Vulnerability of permafrost carbon to
515 climate change: Implications for the global carbon cycle. *BioScience*, 58(8),
516 701–714.
- 517 Schuur, E. A. G., McGuire, A. D., Romanovsky, V., Schädel, C., & Mack, M.
518 (2018). Chapter 11: Arctic and boreal carbon. in second state of the car-
519 bon cycle report (soccr2): A sustained assessment report. In (chap. 11).
520 U.S. Global Change Research Program, Washington, DC, USA. doi:
521 10.7930/SOCCR2.2018.Ch11.
- 522 Schuur, E. A. G., McGuire, A. D., Schädel, C., Grosse, G., Harden, J. W., Hayes,
523 D. J., . . . Vonk, J. (2015). Climate change and the permafrost carbon feed-
524 back. *Nature*, 520, 171-179.
- 525 Swindles, G. T., Morris, P. G., Mullan, D., Watson, E. J., Turner, T. E., Roland,
526 T. P., . . . Galloway, J. M. (2015). The long-term fate of permafrost peat-
527 lands under rapid climate warming. *Scientific Reports*, 5, 17951. doi:
528 DOI:10.1038/srep17951
- 529 Tang, A., & Kemp, L. (2021). A fate worse than warming? stratospheric aerosol in-
530 jection and global catastrophic risk. *Frontiers in Climate*, 3. doi: 10.3389/
531 fclim.2021.720312
- 532 Tarnocai, C., Kettles, I. M., & Lacelle, B. (2011). *Peatlands of canada, open*
533 *file 6561* [report]. Geological Survey of Canada. Retrieved from [https://](https://geoscan.nrcan.gc.ca/starweb/geoscan/servlet.starweb?path=geoscan/fulle.web&search1=R=288786)
534 [geoscan.nrcan.gc.ca/starweb/geoscan/servlet.starweb?path=geoscan/](https://geoscan.nrcan.gc.ca/starweb/geoscan/servlet.starweb?path=geoscan/fulle.web&search1=R=288786)
535 [fulle.web&search1=R=288786](https://geoscan.nrcan.gc.ca/starweb/geoscan/servlet.starweb?path=geoscan/fulle.web&search1=R=288786) doi: 10.4095/288786

- 536 Treat, C. C., Jones, M. C., Adler, J., & Frohking, S. (2022). Hydrologic con-
537 trols on peat permafrost and carbon processes: New insights from past and
538 future modeling. *Frontiers in Environmental Science*, 10(892925). doi:
539 10.3389/fenvs.2022.892925
- 540 Treat, C. C., Jones, M. C., Adler, J., Sannel, A. B. K., Camill, P., & Frohking,
541 S. (2021). Predicted vulnerability of carbon in permafrost peatlands
542 with future climate change and permafrost thaw in western canada. *Jour-
543 nal of Geophysical Research: Biogeosciences*, 126(5), e2020JG005872. doi:
544 10.1029/2020JG005872
- 545 Voigt, C., Marushchak, M. E., Mastepanov, M., Lamprecht, R. E., Christensen,
546 T. R., Dorodnikov, M., . . . Biasi, C. (2019). Ecosystem carbon response
547 of an arctic peatland to simulated permafrost thaw. *Global Change Biology*,
548 25(5), 1746–1764. doi: doi.org/10.1111/gcb.14574
- 549 Wells, J., Roberts, D., Lee, P., Cheng, R., & Darveau, M. (2010). *A forest of blue
550 - canada's boreal forest: The world's waterkeeper*. Seattle: International Boreal
551 Conservation Campaign.
- 552 Zhang, Y., Piao, S., Sun, Y., Rogers, B. M., Li, X., Lian, X., . . . Peñuelas, J. (2022).
553 Future reversal of warming-enhanced vegetation productivity in the northern
554 hemisphere. *Nature Climate Change*, 12, 581–586.